Proposal of ^{BE}SOI MOSFET source sensing region for pH monitoring applications.

Pedro H. Duarte[1], Ricardo C. Rangel[1,2], and Joao A. Martino[1], Senior Member, IEEE.
[1] LSI/PSI/USP, University of Sao Paulo, Sao Paulo, Brazil
[2] FATEC-SP, Faculdade de Tecnologia de Sao Paulo, Sao Paulo, Brazil
E-mail: phduarte@usp.br

***Abstract*— This work presents a study of the sensing regions of ^{BE}SOI MOSFET for pH sensing using TCAD Sentaurus simulation. A new approach was used to model the electrolyte, as previously the device simulator did not have a model for this type of material. The simulation results show an increase in drain current levels for acidic pH values and a decrease for basic pH values. Additionally, the drain voltage demonstrates an influence on the electrolyte charges, which worsens the device sensitivity. Therefore, a new device was proposed, using only the source sensing region to avoid drain influence. This new device shows an improvement in sensitivity, reaching improvement values of 10% up to 72%, and optimizes the obtained results for future experimental analyses.**

***Keywords*—^{BE}SOI MOSFET, pH sensing, Simulation, TCAD.**

I. INTRODUCTION

The Back Enhanced Silicon-On-Insulator MOSFET (^{BE}SOI MOSFET) is a device patented in 2015 [1], as a proposal to design a reconfigurable transistor with less complexity in the fabricating process [2]. The ^{BE}SOI MOSFET is a transistor that does not intentionally contain doped source and drain regions. Fabricated on a SOI (Silicon-On-Insulator) wafer, the silicon film above the buried oxide of the SOI wafer serves as the transistor channel, extending from source to drain, with only natural p-type wafer doping (10^{15} carriers/cm^3). Due to this low doping concentration in the film, there is no current flow between source and drain as there are no doped regions providing the necessary carriers to constitute current. However, because it features an oxide layer (buried oxide) separating the film from the substrate, it is possible to use the voltage applied to the substrate (programming gate) to induce carriers in the channel film. This method, known in the literature [3] as electrostatic doping, refers to carrier induction by an electric field. Therefore, the type and number of carriers are defined by the electric field, allowing a single transistor to function as either a N-type or P-type by simply modifying the applied potential to the substrate.

Initially, this reconfigurability feature was the main focus of research with this device and has been continuously improved upon to this day [4]-[6]. As research progressed, alternative applications were discovered, such as in digital circuits [7] and as certain types of sensors [8][9]. Another significant characteristic of the ^{BE}SOI MOSFET is the presence of Underlap regions, which are spaces between the gate contact and the drain/source contact. These regions are used to evaluate the electrical behavior of the device when subjected to external events, such as light incidence, to function as a light sensor, and with glucose liquid solutions to serve as a biosensor. The application as a biosensor is highly important for contributing to technological development in healthcare, especially in disease monitoring such as diabetes [10], to enhance people's quality of life.

The studies of the ^{BE}SOI MOSFET as a biosensor were initially evaluated through computational simulation environments to verify the feasibility of the idea before experimental implementation. The semiconductor simulator TCAD SENTAURUS was employed for all virtual research, utilizing numerical methods to simulate the electrical effects of the device. TCAD SENTAURUS does not encompass mathematical and physical models for all types of materials, such as liquids, as it is not the focus of this type of simulator. Hence, the simulations were initially adapted in a simplified manner to represent biological material in the sensing regions, like using an oxide with the dielectric constant of water ($k_{water}=80\varepsilon0$) with different amounts of effective charges [11] to assess the influence of charges in these areas, and an approach to evaluate various dielectric constants with values corresponding to certain types of biological materials (including glucose) [12].

These initial simulations greatly contributed to understanding the influences of biological material in these regions on the electrical behavior of the device, which aligned with experimental results showing similar trends to those simulated. As this was a simplistic but effective approach, efforts are underway to improve aspects of the simulation to make them more realistic. Therefore, this work presents a study of the sensing regions of the ^{BE}SOI MOSFET in a simulation environment with an alternative approach to representing the electrolyte in a semiconductor simulation.

II. SIMULATION CHARACTERISTICS

A. *Electrolyte Model*

A simulation study was conducted using the TCAD SENTAURUS tool to assess charge distribution in the electrolyte. The simulation was carried out based on a methodology previously outlined in relevant literature [13]. Since TCAD lacks an appropriate model for electrolytes/solutions, the adopted approach involved a definition of the solution as an intrinsic semiconductor with a relative dielectric constant equivalent to that of water ($k_{water}=80\varepsilon0$).

Considering pure water at 25°C, the dissociation of water molecules tends to maintain the ionization product in equilibrium ($Kw = 10^{-14}$ mol²/L²). If the pH of water is 7, the pOH will also be 7, meaning both the concentrations of H+ and OH- ions will be equal to 10^{-7} mol/L. If the pH changes, the ion concentrations are adjusted to always keep the ionization product constant. This characteristic is very similar to the properties of intrinsic silicon in thermal equilibrium, where the product of the number of carriers in the semiconductor, holes (p), and electrons (n), is always constant ($p.n = ni^2$). Therefore, it is possible to approach adapting the electrolyte model for the simulator.

To calculate the quantity of carriers in the electrolyte to feed into the simulator, it is assumed that the concentration of H^+ ions, [H^+], is equal to the concentration of holes in the semiconductor, and the concentration of OH^- ions, [OH^-], is equal to the concentration of electrons in the semiconductor. With this, it is possible to use Avogadro's number (6.022×10^{23}) to determine the number of ions per cm³ in a pH solution and estimate how many carriers need to exist in each case for the semiconductor to function as an electrolyte. The simulator uses standard equations to determine the quantity of carriers in silicon, equations that depend on the density of states, requiring the modification of model parameters for each pH value.

B. *Device Characteristic*

The [BE]SOI MOSFET was simulated using a Silicon-On-Insulator (SOI) substrate with intrinsic doping of $1x10^{15}$ carriers per cm³. From the transistor dimensions, the gate length (L) was defined as 1 µm, and for a 2D simulation, the gate width (W) was also set to 1 µm. The thicknesses of the gate oxide (t_{ox}), channel silicon layer (t_{Si}), buried oxide (t_{BOX}), the electrolyte and the substrate are, respectively, 10nm, 20nm, 200nm, 500nm and 1 µm. The sensitive regions have a length of 500 nm, and it is in this region that the defined model will be implemented in this work. Fig. 1A shows a 3D schematic drawing to provide an idea of how the device would appear if fabricated, while Fig. 1B depicts a schematic cross-sectional profile of the device, which was used for the 2D simulation.

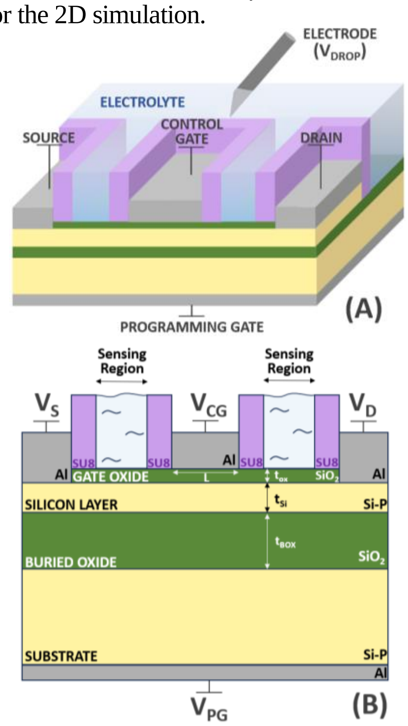

Fig. 1. Device schematic drawing on 3D (A) and 2D (B) view of [BE]SOI MOSFET showing the sensing regions, where V_S is the voltage represents the source voltage; V_D is the drain voltage; V_{DROP} is the electrolyte voltage; V_{CG} is the control gate voltage and V_{PG} is the programming gate voltage.

III. RESULTS AND ANALYSIS

To commence the study of the electrical behavior of the device, the $I_{DS}xV_{GS}$ curve was obtained, as shown in Fig. 2.

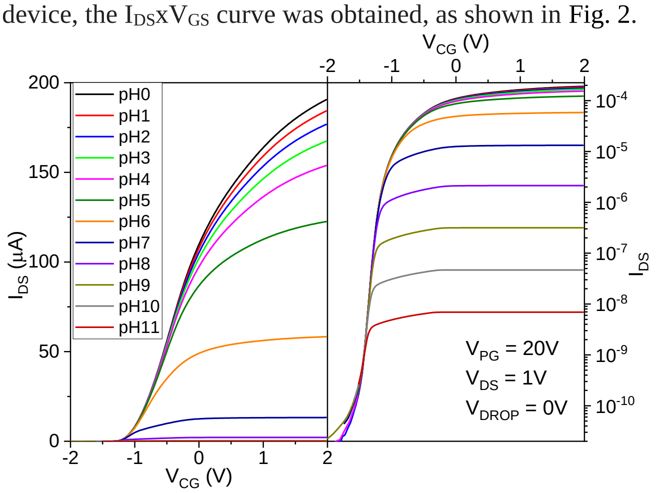

Fig. 2. Drain current as a function of the control gate voltage for different pH values on a linear (left) and logarithmic (right) scale.

In the curve, it is possible to observe different levels of current for various pH values. For more acidic values, the current increases, whereas for more basic values, the current tends to decrease. This phenomenon occurs due to the geometry of the device. Yojo [12] modeled the sensitive area as transistors connected in series along with a main transistor controlled by the gate. In other words, there is an arrangement of three transistors in series: one main transistor controlled by the gate and two secondary transistors controlled by the voltage applied to the electrode of the liquid in the sensitive area, as shown in Fig. 3.

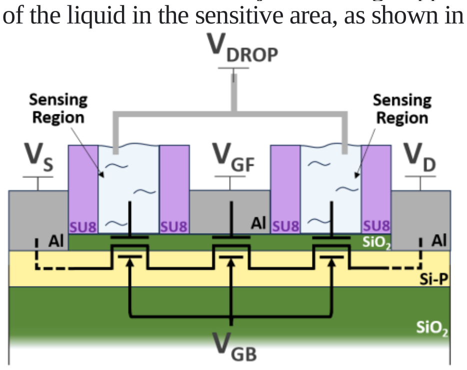

Fig. 3. [BE]SOI MOSFET device electric model

In addition to extracting the current level as a function of the gate voltage, other investigations were conducted. It was observed that the voltage applied to the electrode, V_{DROP}, could contribute to increasing or decreasing the device current. Fig. 4 shows the electron density for pH2 (very acidic) and pH10 (very basic), with electrode applied voltages of 0.0V and 0.9V in the sensitive region near the Drain. This analysis was carried out to aid in understanding the obtained results and to examine the effect of potential in the electrolyte

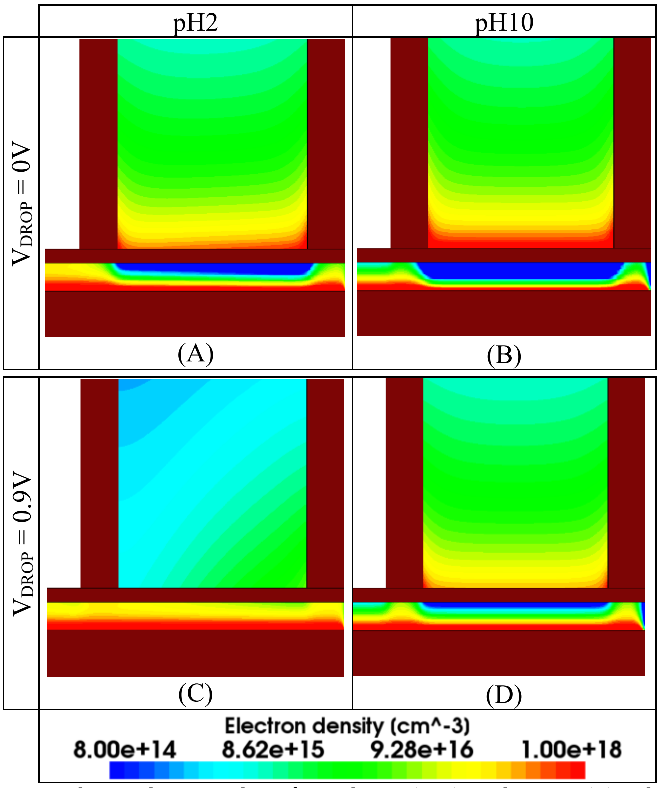

Fig. 4. Electron density analyses for acidic pH (pH2), applying 0V (A) and 0.9V (B) to the electrolyte (V_{DROP}) and basic pH (pH10) for the same voltage values, 0V (C) and 0.9V (D).

From the images presented in the table, it is evident that for a more acidic pH (pH2), there is a lower electron density compared to a more basic pH (pH10), which was expected based on the used model. The attraction of these carriers to the electrolyte/oxide interface is due to the distributed channel potential up to the electrode applying voltage to the electrolyte, causing a departure of the majority carriers (in this case, electrons) from the channel at the oxide/channel interface, thereby impeding current flow through that region. This leads to an increase in series resistance, resulting in decreased current for higher pH values. If the applied voltage to the electrolyte increases, the potential difference between the electrolyte and the channel decreases, attracting fewer electrons to the electrolyte/oxide interface, reducing the series resistance, and increasing the current. Fig. 5 illustrates the potential distribution from the substrate to the electrode in the active region near the drain.

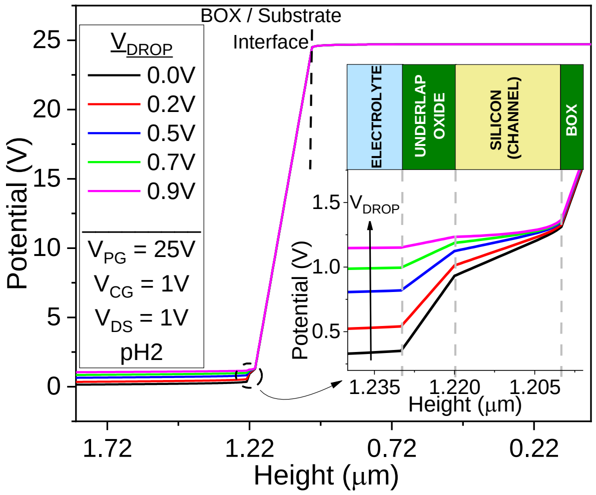

Fig. 5. The drain sensing structure potential analysis for different electrolyte applied voltage (V_{DROP}).

As mentioned earlier, the table was compiled using data obtained from the sensitive area near the Drain. This was done because it was noticed that for acidic pH values and higher V_{DROP} voltages, the potential difference between the electrolyte and the channel near the drain was small but non-uniform. In the table, it can be observed that for pH2 with V_{DROP} of 0.9V, there is a higher concentration of electrons moving towards the drain contact. This electron concentration leads to an increase in series resistance, which worsens the current level for acidic pH values, as the electron density is much higher for more basic pH values and the influence of the drain is minimal.

Based on this, the study of the ^{BE}SOI MOSFET with only one sensitive area, on the Source side, was proposed, as shown in the schematic diagram in Fig. 6. With this area near the Source, the charges in the electrolyte will only be influenced by the voltage applied to the Source, which will be at 0V.

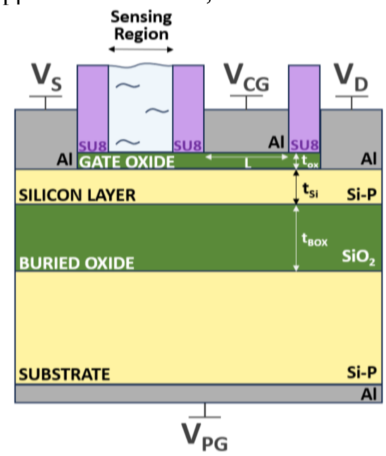

Fig. 6. 2D schematic drawing of the new device proposal, the ^{BE}SOI MOSFET source sensing region.

Similarly to the evaluation conducted on the device with two sensitive regions, the current value (I_{DS}) was extracted as a function of the control gate voltage (V_{CG}), as depicted in the graph in Fig. 7.

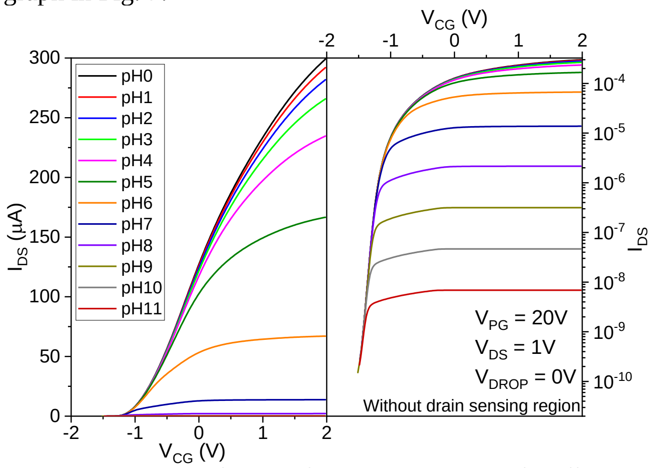

Fig. 7. Drain current as a function of the control gate voltage for different pH values for the new device proposal.

In the figure, it can be observed that the device exhibits the same characteristic as the first device but with higher current levels. This is due to the absence of the sensitive region near the drain, eliminating one of the secondary transistors that can limit the current and, consequently, reducing the series resistance and increasing the current level.

To compare the devices, a sensitivity metric (S) was defined. To calculate this sensitivity, a gate voltage value of 1.5V was chosen, and the corresponding current level was verified. The reference current chosen is for pH7, which represents the neutral state of the electrolyte. Therefore, the value of S for each pH is obtained using (1): the absolute difference between the current at a pH value ($I_{DS_{pH}}$) and the reference current ($I_{DS_{ref}}$), divided by the reference current.

$$|S| = \left|\frac{(I_{DS_{pH}} - I_{DS_{ref}})}{I_{DS_{ref}}}\right| \tag{1}$$

Therefore, the comparison between devices is presented in Fig. 8 for different values of applied programming gate voltage, along with the comparison of the sensitivities achieved in each case shown in the graph inset.

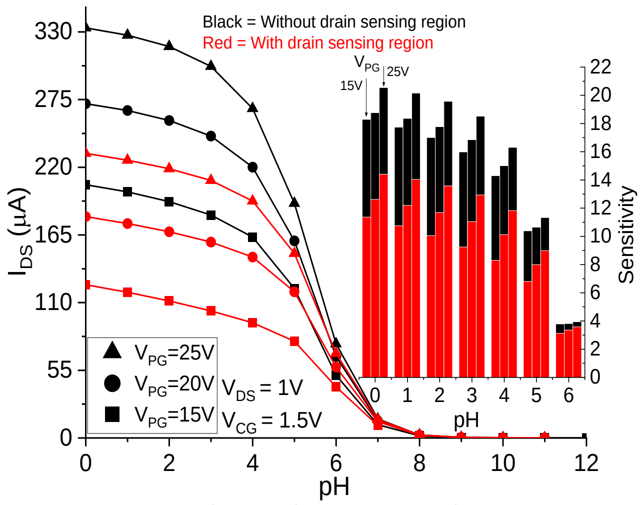

Fig. 8. Drain current as a function of pH value at 1.5V for control gate voltage, and sensitivity analyses for which device.

In the graph presented, it can be observed that for pH values greater than 7, regardless of the device used, the current levels are very low, resulting in sensitivities that are close to 1, which is the lowest possible level. For pH values greater than 7, the sensitivity achieves more noticeable values, increasing as the applied programming gate voltage changes. This occurs due to the electrostatic coupling of the transistor, where increasing this voltage will increase the number of carriers available in the channel, thereby reducing the series resistance and increasing sensitivity. Additionally, the red curves demonstrate that sensitivity is lower when the transistor has the sensitive region near the drain, as it is influenced by the voltage applied to the drain. Removing this region, indicated by the black lines, eliminates the drain's influence on the charges, removing a parameter that affects sensitivity.

After determining the optimal geometric configuration of the device, specifically without the drain region, the influence of the voltage applied to the electrolyte was investigated, as shown in Fig. 9.

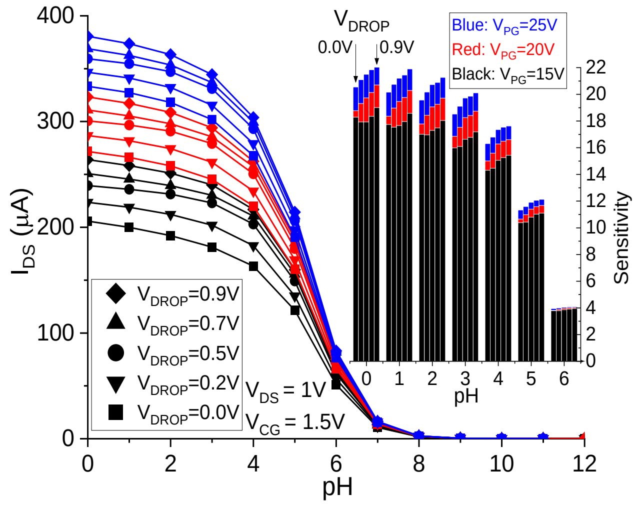

Fig. 9. Drain current as a function of pH for the device without drain sensing region, and sensitivity analyses for which electrolyte voltage.

The graphs show that increasing the voltage applied to the electrolyte leads to an increase in current and sensitivity. As shown in Fig. 5, the voltage applied to the electrolyte contributes to reducing the series resistance of the transistor, further enhancing sensitivity. This aligns with the results presented in Fig. 9.

IV. CONCLUSIONS

This study presented the implementation of a model for electrolytes via simulation using TCAD Sentaurus. This model was used to optimize the investigation into the electrical behavior of the ^{BE}SOI MOSFET as a biosensor. The sensitive Source and Drain regions were analyzed with simulated pH values obtained from the model. Variation in pH values showed an increase in current for more acidic conditions and a decrease for more basic conditions. It was observed that the Drain voltage interferes with the interaction of charges in the electrolyte with charges in the channel. Therefore, a new device was proposed with only one sensitive region at the source region. This device demonstrated increased sensitivity in all cases, reaching improvement values of 10% up to 72%.

Based on the results presented in this study, it will be possible to define optimal working points for conducting experimental work using the ^{BE}SOI MOSFET as an optimized pH sensor.

ACKNOWLEDGMENT

The authors acknowledge CNPq, CAPES and São Paulo Research Foundation - FAPESP (under grant #2020/04867-2) for the financial support.

REFERENCES

[1] J. A. Martino and R. C. Rangel, "Método de Fabricação de Transistor," patent number BR102015020974-6, 2015.

[2] R. C. Rangel and J. A. Martino, "Back Enhanced (BE) SOI pMOSFET," in *2015 30th Symposium on Microelectronics Technology and Devices (SBMicro)*, Salvador, Brazil: IEEE, Aug. 2015, pp. 1–4. doi: 10.1109/SBMicro.2015.7298121.

[3] G. Gupta, B. Rajasekharan, and R. J. E. Hueting, "Electrostatic Doping in Semiconductor Devices," *IEEE Trans. Electron Devices*, vol. 64, no. 8, pp. 3044–3055, Aug. 2017, doi: 10.1109/TED.2017.2712761.

[4] D. A. Ramos, K. R. A. Sasaki, R. C. Rangel, P. H. Duarte, and J. A. Martino, "Influence of the source/drain doping region on the reconfigurability of ^{BE} SOI MOSFET," in *2023 37th Symposium on Microelectronics Technology and Devices (SBMicro)*, Rio de Janeiro, Brazil: IEEE, Aug. 2023, pp. 1–4. doi: 10.1109/SBMicro60499.2023.10302644.

[5] H. L. Carvalho, R. C. Rangel, K. R. A. Sasaki, P. G. D. Agopian, L. S. Yojo, and J. A. Martino, "Al Source-Drain Schottky contact enabling N-type (Back Enhanced) ^{BE} SOI MOSFET," in *2022 36th Symposium on Microelectronics Technology (SBMICRO)*, Porto Alegre, Brazil: IEEE, Aug. 2022, pp. 1–4. doi: 10.1109/SBMICRO55822.2022.9880960.

[6] R. A. Sasaki, R. C. Rangel, D. A. Ramos, L. S. Yojo, and J. A. Martino, "Improved Back Enhanced SOI (^{BE} SOI) MOSFET by adding n-doped regions," in *2021 35th Symposium on Microelectronics Technology and Devices (SBMicro)*, Campinas, Brazil: IEEE, Aug. 2021, pp. 1–4. doi: 10.1109/SBMicro50945.2021.9585735.

[7] L. Yojo, R. C. Rangel, K. R. A. Sasaki, and J. A. Martino, "Reconfigurable back enhanced (BE) SOI MOSFET used to build a logic inverter," in *2017 32nd Symposium on Microelectronics Technology and Devices (SBMicro)*, Fortaleza: IEEE, Aug. 2017, pp. 1–4. doi: 10.1109/SBMicro.2017.8112987.

[8] J. A. Padovese, R. C. Rangel, K. R. A. Sasaki, and J. A. Martino, "Thin Si channel Back Enhanced (BE) SOI pMOSFET Photodetector under different bias conditions," in *2019 Joint International EUROSOI Workshop and International Conference on Ultimate Integration on Silicon (EUROSOI-ULIS)*, Grenoble, France: IEEE, Apr. 2019, pp. 1–4. doi: 10.1109/EUROSOI-ULIS45800.2019.9041870.

[9] L. S. Yojo, R. C. Rangel, K. R. A. Sasaki, and J. A. Martino, "Study of ^{BE} SOI MOSFET Reconfigurable Transistor for Biosensing Application," *ECS J. Solid State Sci. Technol.*, vol. 10, no. 2, p. 027004, Feb. 2021, doi: 10.1149/2162-8777/abe3cc.

[10] A. Heller and B. Feldman, "Electrochemical Glucose Sensors and Their Applications in Diabetes Management," *Chem. Rev.*, vol. 108, no. 7, pp. 2482–2505, Jul. 2008, doi: 10.1021/cr068069y.

[11] L. S. Yojo, R. C. Rangel, K. R. A. Sasaki, C. A. Mori, and J. A. Martino, "Optimization of the Back Enhanced ^{BE} SOI MOSFET working as a charge-based BioFET sensor," in *2019 IEEE SOI-3D-Subthreshold Microelectronics Technology Unified Conference (S3S)*, San Jose, CA, USA: IEEE, Oct. 2019, pp. 1–3. doi: 10.1109/S3S46989.2019.9320714.

[12] L. S. Yojo, R. C. Rangel, K. R. A. Sasaki, and J. A. Martino, "Optimization of the permittivity-based BE SOI biosensor," in *2018 IEEE SOI-3D-Subthreshold Microelectronics Technology Unified Conference (S3S)*, Burlingame, CA, USA: IEEE, Oct. 2018, pp. 1–3. doi: 10.1109/S3S.2018.8640139.

[13] R. Narang, M. Saxena, and M. Gupta, "Analytical Model of pH sensing Characteristics of Junctionless Silicon on Insulator ISFET," *IEEE Trans. Electron Devices*, vol. 64, no. 4, pp. 1742–1750, Apr. 2017, doi: 10.1109/TED.2017.2668520.